論文 / 著書情報
Article / Book Information

Title	Concurrent x-ray diffractometer for high throughput structural diagnosis of epitaxial thin films
Authors	M. Ohtani,T. Fukumura,M. Kawasaki,K. Omote,T. Kikuchi,J. Harada,A. Ohtomo,M. Lippmaa,T. Ohnishi,D. Komiyama,R. Takahashi,Y. Matsumoto,H. Koinuma
Citation	Applied Physics Letters, Vol. 79, No. 22,
Pub. date	2001, 11
URL	http://scitation.aip.org/content/aip/journal/apl
Copyright	Copyright (c) 2001 American Institute of Physics

Concurrent x-ray diffractometer for high throughput structural diagnosis of epitaxial thin films

M. Ohtani[a)]
Department of Innovative and Engineered Materials, Tokyo Institute of Technology, Yokohama 226-8502, Japan

T. Fukumura and M. Kawasaki[b)]
Institute for Materials Research, Tohoku University, Sendai 980-8577, Japan

K. Omote, T. Kikuchi, and J. Harada
X-Ray Research Laboratory, Rigaku Corporation, Tokyo 196-8666, Japan

A. Ohtomo, M. Lippmaa, T. Ohnishi, D. Komiyama, R. Takahashi, Y. Matsumoto, and H. Koinuma[b),c)]
Frontier Collaborative Research Center and Materials and Structures Laboratory, Tokyo Institute of Technology, Yokohama 226-8503, Japan

(Received 11 June 2001; accepted for publication 27 August 2001)

We have developed a concurrent x-ray diffractometer that concurrently measures spatially resolved x-ray diffraction (XRD) spectra of epitaxial thin films integrated on a substrate. A convergent x-ray is focused into stripe on a substrate and the diffracted beam is detected with a two-dimensional x-ray detector. The obtained snapshot image represents a mapping of XRD intensity with the axes of the diffraction angle and the position in the sample. In addition to the parallel XRD measurements of thin films with various compositions and structures, two-dimensional spatial mapping of XRD peak with a resolution of $\sim 100\,\mu$m is demonstrated. This technique will provide us a high throughput characterization method of various devices composed of epitaxial films. © *2001 American Institute of Physics.* [DOI: 10.1063/1.1415402]

Recently, parallel synthesis of solid-state thin films having electronic, magnetic, and optical functionalities based on combinatorial methodology has attracted much attention for efficient materials discovery.[1,2] Strong demands are focused on high throughput characterization of thin film libraries integrated on substrates. Dielectric, magnetic, and optical characterizations have been demonstrated by microwave microscope,[3] scanning superconducting quantum interference device microscope,[4] and spectroscopic microscope,[5] respectively. However, adoption of conventional tool to combinatorial libraries for the structural characterization such as x-ray diffraction has been difficult. Isaacs *et al.* reported on a sophisticated characterization tool of combinatorial libraries by using focused x-ray beam from synchrotron orbital radiation source.[6] Not only the diffraction but also the fluorescence and absorption spectroscopy have been demonstrated to characterize the structure and chemical state of library. However, the use of synchrotron orbital radiation source is considerably limited. Here, we report on a high throughput structural characterization technique for epitaxial thin film library integrated on a substrate suitable for laboratory use by using an x-ray diffraction (XRD) apparatus having rotating anode source, special x-ray optics and x-ray charge-coupled-device (CCD), named as concurrent XRD (CXRD). The spatially resolved XRD spectra are taken in a very short time to map out the structure and crystallinity of thin film libraries.

Figure 1 shows a schematic diagram of the CXRD. An x-ray beam with a diameter of about 100 μm is produced from a rotating copper anode fine-focus x-ray generator (1.2 kW). A Johan-type curved monochromator is used to eliminate $\mathrm{Cu}K\alpha_2$, $\mathrm{Cu}K\beta$, and white radiation and to focus $\mathrm{Cu}K\alpha_1$ divergence beam into an area of ~ 10 mm $\times 100\,\mu$m on the sample surface with the convergence angle of 2°. The sample and CCD camera are mounted on the ω and 2θ stage of conventional two-circle goniometer, respectively. The diffracted beam is imaged on the CCD camera, where the two axes of image correspond to the position in the sample and the 2θ angle. The spatial resolution of the image is limited by the diameter of x-ray beam for both axes in the present geometry. The measurement time varies from 5 s to a few minutes.

Figure 2(a) shows a CXRD image of five superlattices $[(SrTiO_3)_n/(BaTiO_3)_4]_{30}$ ($n=2$, 4, 6, 8, 10) integrated on $SrTiO_3$ (001) substrate as illustrated in Fig. 2(c). The sample was prepared by *in situ* monitoring the intensity oscillation of reflection high energy electron diffraction for all the superlattices simultaneously with a combinatorial pulse laser deposition system.[7] The layer thickness was controlled by a stencil mask adjacent to the substrate. The mask position was slid synchronously with the oscillation of reflection high energy electron diffraction. The vertical straight line in Fig. 2(a) is (001) diffraction peak from the $SrTiO_3$ substrate, and the adjacent lines with steps correspond to the fundamental and satellite peaks of each superlattice. The 2θ values of the fundamental peaks shift owing to the change in averaged lattice constants of superlattices. The systematical shift of

a)Electronic mail: ohtani@oxide.rlem.titech.ac.jp
b)Also at Combinatorial Materials Exploration and Technology (COMET).
c)Also at CREST, Japan Science and Technology Corporation.

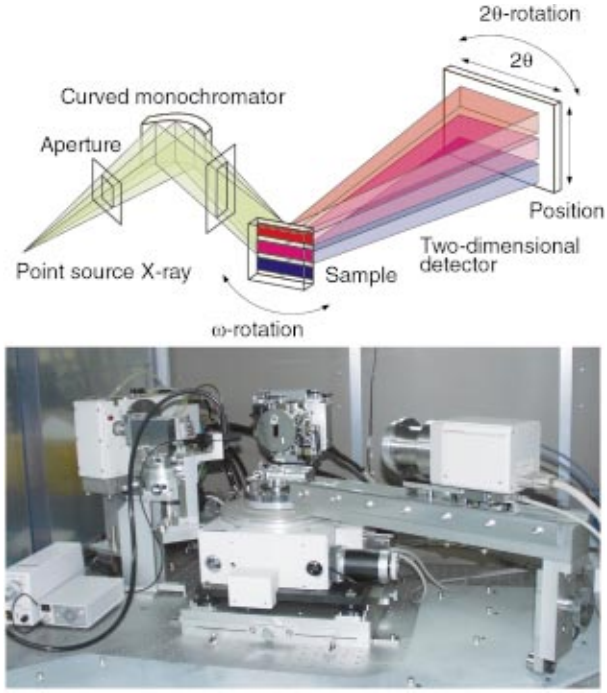

FIG. 1. (Color) Schematic diagram (top) and a photograph (bottom) of CXRD. The x-ray beam is focused by a Johan-type monochromator to form a convergent beam of $\sim 10\,\text{mm} \times 100\,\text{mm}$ with a convergence angle of 2° on the sample. The sample and the CCD camera for two-dimensional x-ray detector are mounted on the ω and 2θ stages of the two-circle goniometer, respectively. The diffracted beam is imaged on the CCD camera with axes of diffraction angle 2θ and position in the sample.

satellite peaks corresponds to the change in superlattice periods. By taking cross sections of the Fig. 2(a) for each superlattice, one can extract the conventional XRD patterns as shown in Fig. 2(b), that have to be measured serially with a conventional XRD measurement system.

Figure 3(a) shows a CXRD image for a composition-spread film of $Ba_xSr_{1-x}TiO_3$ ($0 \leqslant x \leqslant 1$) on $SrTiO_3$ (001) substrate. While $SrTiO_3$ and $BaTiO_3$ ceramics targets were alternately ablated, two masks were synchronously slid so

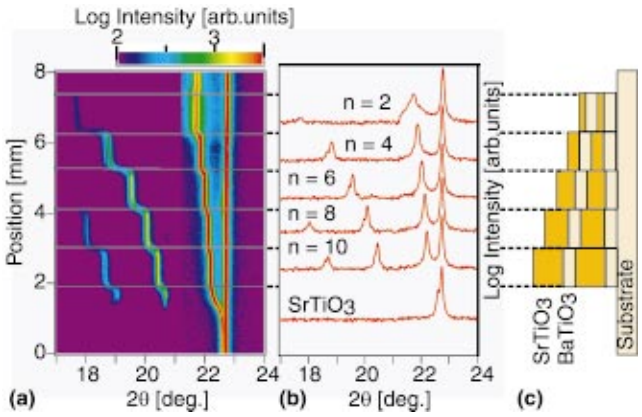

FIG. 2. (Color) (a) CXRD image of five superlattices $[(SrTiO_3)_n/(BaTiO_3)_4]_{30}$ ($n=2$, 4, 6, 8, 10) (from 70 to 170 nm thick) integrated on $SrTiO_3$ (001) substrate. The vertical and horizontal axes correspond to the position in the film and the diffraction angle 2θ, respectively. The color denotes logarithmic XRD intensity. The vertical straight line and the adjacent lines with steps represent the XRD peak of the substrate (001) and the superlattices, respectively; (b) the horizontal cross sections of (a) at each superlattice corresponding to the conventional XRD spectra; (c) a schematic cross section of the sample.

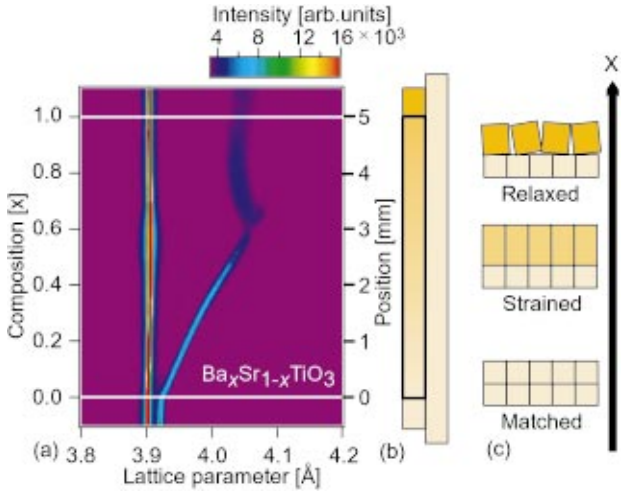

FIG. 3. (Color) (a) CXRD image of composition-spread film $Ba_xSr_{1-x}TiO_3$ ($0 \leqslant x \leqslant 1$) (200 nm thick) on $SrTiO_3$ (001) substrate. The vertical and horizontal axes correspond to x and 2θ, respectively. The color denotes logarithmic XRD intensity.

that the x value was linearly changed along the position in the film. The areas below 0 mm and above 5 mm are pure $SrTiO_3$ and $BaTiO_3$ films, as shown in Figs. 3(a) and 3(b), respectively. The vertical straight line and the adjacent curve are (002) peaks of substrate and film, respectively.[5] As x increases the volume of film expands owing to the substitution of Ba for Sr, however, the in-plane lattice constant is the same as that of substrate up to $x=0.6$ due to the epitaxial strain from the substrate. Consequently, the out of plane lattice constant increases with increasing x accompanied by the tetragonal lattice distortion as illustrated in the middle of Fig. 3(c). As x increases over 0.6, the out-of-plane lattice constant decreases abruptly since the compressive stress is relaxed by the generation of misfit dislocations at the interface between film and substrate as illustrated at the top of Fig. 3(c). This result clearly demonstrates a limit of the coherent epitaxial growth on the lattice-mismatched substrate as a function of degree of lattice mismatch. In addition, the lattice constant and mosaicity can be mapped out as a function of the posi-

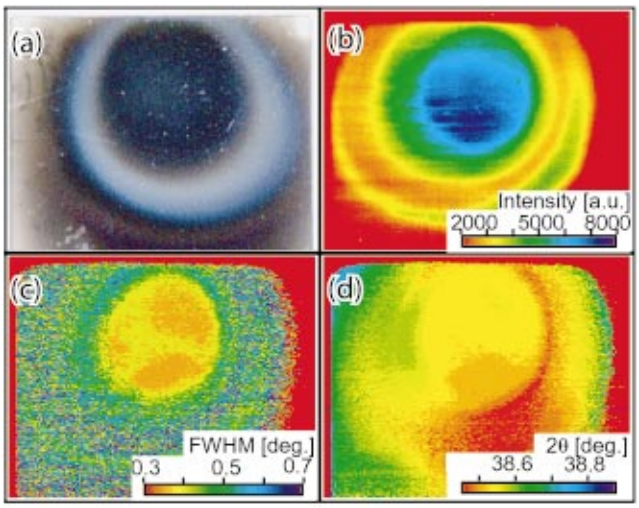

FIG. 4. (Color) (a) Photograph of $YBa_2Cu_3O_{7-\delta}$ film (800 nm) on $SrTiO_3$ (001) substrate. (b) XRD intensity; (c) FWHM; and (d) 2θ of (005) peak of film are mapped out on the same area as (a).

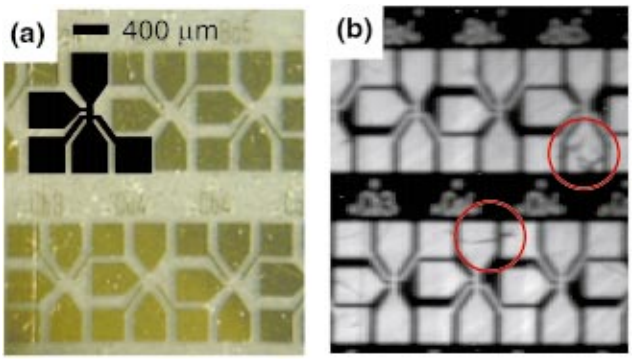

FIG. 5. (Color) (a) Photograph of Hall bar array made of transparent ZnO film (900 nm thick) on transparent $ScAlMgO_4$ substrate. The Hall bars are invisible except for the gold electrodes (100 nm thick). Inset shows the pattern of the Hall bar; (b) XRD intensity mapping for (004) peak of film. The gray scale denotes XRD intensity. The microscopic crystal defects are seen in red circles.

tion or x, by using the values of the 2θ and the full width at half maximum (FWHM) from Figs. 2 and 3.

By sliding the sample translationally, one can map out the crystallinity of the entire film in two-dimension. Figure 4(a) shows an image of a $YBa_2Cu_3O_{7-\delta}$ film that has intentional inhomogeneity caused by an unoptimized condition of pulsed laser deposition. Figures 4(b)–4(d) show the mapping results of XRD intensity, FWHM, and peak position of the (005) peak, respectively. This mapping is deduced from 160 measurements accompanied by the translation of sample with each increment of 100 μm. The film shows excellent crystallinity at the center as depicted in Figs. 4(b) and 4(c). However, the film has elongated lattice constant in Fig. 4(d) as indicated by the red color around the right bottom. This is presumably due to Y–Ba substitution caused by slight off-stoichiometry.[8] The conventional XRD cannot be as useful as CXRD for the optimization of pulsed laser deposition parameters.

The mapping of XRD intensity as shown in Fig. 4 is useful for the inspection of epitaxial thin film devices as well. Figure 5(a) shows a photograph of Hall bar array made of transparent conducting ZnO film on $ScAlMgO_4$ substrate.[9] The inset of Fig. 5(a) shows the pattern of the Hall bar. The Hall bar is invisible by the naked eye except for the gold electrodes on the bar. Figure 5(b) shows the XRD intensity mapping of the same Hall bar array by a similar measurement in the case of Fig. 4. The whole Hall bars are clearly visualized including parts beneath gold electrode with 100 nm thick. Several dark areas in red circles are thought to represent existence of microscopic crystal defects, that cannot be seen with an ordinary microscope.

In conclusion, we have developed CXRD that measures spatially resolved XRD spectra along a 10 mm line on a substrate with a resolution of about 100 μm. High throughput characterization of combinatorial epitaxial thin film libraries is demonstrated. With the translational scan of the sample, XRD microscopy is performed to map out the crystallinity of the film and the device configuration.

This work was supported by JSPS Research for the Future Program in the area of Atomic-Scale Surface and Interface Dynamics (RFTF96P00205) and Proposal Based Program of NEDO (99S12010).

[1] X.-D. Xiang, X. Sun, G. Briceno, Y. Lou, K.-A. Wang, H. Chang, W. G. Wallace-Freedman, S.-W. Chen, and P. G. Schultz, Science **268**, 1738 (1995).
[2] Y. Matsumoto, M. Murakami, Z. Jin, A. Ohtomo, M. Lippmaa, M. Kawasaki, and H. Koinuma, Jpn. J. Appl. Phys., Part 2 **38**, L603 (1999).
[3] H. Chang, C. Gao, I. Takeuchi, Y. Yoo, J. Wang, P. G. Schultz, X.-D. Xiang, R. P. Sharma, M. Downes, and T. Venkatesan, Appl. Phys. Lett. **72**, 2185 (1998).
[4] Y. Matsumoto, M. Murakami, T. Shono, T. Hasegawa, T. Fukumura, M. Kawasaki, P. Ahmet, T. Chikyow, S. Koshihara, and H. Koinuma, Science **291**, 854 (2001).
[5] T. Fukumura, Y. Okimoto, M. Ohtani, T. Kageyama, T. Koida, M. Kawasaki, T. Hasegawa, Y. Tokura, and H. Koinuma, Appl. Phys. Lett. **77**, 3426 (2000).
[6] E. D. Isaacs, M. Marcus, G. Aeppli, X.-D. Xiang, X. Sun, P. G. Schultz, H.-K. Kao, G. S. Cargill III, and R. Haushalter, Appl. Phys. Lett. **73**, 1820 (1998).
[7] The fabrication procedure of the sample is described in: T. Ohnishi, D. Komiyama, T. Koida, S. Ohashi, A. Ohtomo, M. Lippmma, N. Nakagawa, C. Stauter, T. Kikuchi, K. Omote, M. Kawasaki, and H. Koinuma, Appl. Phys. Lett. **79**, 536 (2001).
[8] J. P. Gong, M. Kawasaki, K. Fujito, R. Tsuchiya, M. Yoshimoto, and H. Koinuma, Phys. Rev. B **50**, 3280 (1994).
[9] A. Ohtomo, K. Tamura, K. Saikusa, K. Takahashi, T. Makino, Y. Segawa, H. Koinuma, and M. Kawasaki, Appl. Phys. Lett. **75**, 2635 (1999).